Egypt. J. Chem. **Vol. 67**, No. 12 pp. 157 - 166 (2024)

Egyptian Journal of Chemistry

http://ejchem.journals.ekb.eg/

Anti-Hepatocellular and anti-lung Carcinoma Effect of the Selenium Nanoparticles Myco-Synthesized by *Penicillium citrinum*: An *in Vitro* Study

Marwa K. Aly[a*], A. F. El-Baz[b], Abdel Hady A. Abdel Wahab[c], Amal A. I. Mekawey[d], Ebtehag A.E. Sakr[e*], Mehreshan T. El-mokadem[e]

[a]*Central Laboratory,Ministry of Environment, Cairo 11728, Egypt*
[b]*Department of Industrial Biotechnology, Genetic Engineering and Biotechnology Research Institute, University of Sadat City, Sadat City 32897, Egypt*

[c]*Cancer Biology Department, National Cancer Institute, Cairo University,Cairo11796, Egypt*

[e]*The regional center of mycology and biotechnology, Al Azhar University, Cairo 11787, Egypt*

[e]*Botany Department, Faculty of Women for Arts, Science and Education, Ain Shams University, Cairo 11757, Egypt*

Abstract

In the current study, biogenic selenium nanoparticles (Se-NPs) were extracellularly synthesized by *Penicillium citrinum*. Se-NPs were structurally and morphologically characterized by using analytical techniques such as: X-ray diffraction (XRD), UV-Vis spectroscopy, Fourier Transform Infrared Spectroscopy (FTIR) and transmission electron microscopy (TEM). Maximum UV absorbance was obtained at 255 nm. and the TEM showed 15–40 nm-sized homogeneous spherical Se-NPs. Anticancer potential of the Se-NPs was evaluated against lung cancer (A-459), hepatocellular carcinoma (HepG2), and its cytotoxicity against normal fibroblast cells (WI-38). The Se-NPshave a significant cytotoxic effect (IC_{50}) of 100.2 ± 3.28 µg/mL against HepG2 cells and IC_{50} of 142.5 ± 6.91 µg/mLagainst A-549 cells, whereas it has IC_{50} of 219.75 ± 10.93 µg/mL against Wl-38 cells. In comparison to the untreated HepG2 cells, the treated cells showed a 1.8 and 1.7-fold increase in superoxide dismutase enzyme(SOD) and glutathione (GSH) content, respectively, with a 0.6 fold drop in catalase (CAT) level. The cell apoptosis rates were also assesed using the Annexin V-FITC staining test. In the treated cells, the rates of necrosis, late apoptosis, and early apoptosis were all markedly elevated. The caspase-3 enzyme level of the treated cells was 2.2 folds higher than that of the untreated cells. Flow cytometer showed an arrest in G2/M phase in comparison to untreated cells after treatment of HepG2 with Se-NP. In conclusion, the biogenic Se-NPs exhibited anticancer activity against HepG2 hepatocellular carcinoma cells through enhanced antioxidant production, apoptosis, and cell cycle arrest pathways.

Keywords: Selenium Nanoparticles; Hepatocellular carcinoma; antioxidant enzymes; Apoptosis; *Penicillium citrinum*

1. Introduction

There are many uses for the biologically produced nanoparticles, such as food preservatives [1], quantum dot nanoparticles [2], anticancer and antibacterial [3], and also bioremediation of heavy metals [4].Selenium is an essential trace element and has a variety of biological functions, where it was used as supplementation of the diet with 0.2 mg of Se-NPs is sufficient to improve ruminal digestibility and fermentation [5].The Use of nano-Se medication in the therapy of Huntington's disease has given promising results [6].SeNPs possess unique semiconducting, photoelectric, and X-ray-sensing properties, and are used in photocells, photocopying, photometers, and xerography [7]Their importance in renewable energy devices has also been greatly mentioned [8]**.**Additionally, selenium nanoparticles (SeNPs) are environmentally important because of their mercury-capturing properties. [9]. Many of the problems with conventional

*Corresponding author e-mail: marwakhirat@yahoo.com.; (Marwa K. Aly).
EJCHEM use only: Received date 18 March 2024; revised date 06 May 2024; accepted date 06 May 2024
DOI: 10.21608/EJCHEM.2024.277342.9464

pharmaceutical formulations can be resolved by using nanotechnology [10]. When it comes to the high specificity, sensitivity, and efficacy of cancer treatment and detection, customized nanomaterials have come a long way [11]. Additionally, it offers concurrent cancer diagnosis and therapy with the use of nano-theragnostic particles, which enable early identification and targeted cancer cell annihilation [12]. The fundamental principle governing nanomaterials is that they possess optical, structural, or magnetic characteristics absent from molecules or bulk substances [13].

Numerous epidemiological, preclinical, and clinical investigations have shown that selenium (Se), the mineral trace element, is vital to both humans and animals, plays a significant role in cancer cells and functions as a chemotherapeutic and chemo preventive agent [13]. Due to its pro- and anti-oxidative properties, selenium is one of the essential minerals for preserving the health of mammalian animals. Se-NPs have been shown to exhibit low toxicity and high biological activity in medicine [14].In the past, Se-NPs have garnered more interest because of their low toxicity and antioxidant properties [15]. In addition to being more biocompatible and having more anticancer activity than inorganic or organic selenium compounds, Se-NPs are also gaining more and more attention as agents for cancer prevention or as nano-carriers of medications or genes for cancer therapy [16]. Se-NPs may have anticancer effects through enhancing immunity [17], inducing cell-cycle arrest, inducing apoptosis via the intrinsic or mitochondrial-dependent mechanism, or via the extrinsic or death receptor pathway [16]. Numerous investigations demonstrated that Se-NPs possesses both *in vivo* and *in vitro* antioxidant properties by activating selenoenzymes such thioredoxin reductase (TrxR) and glutathione peroxidase (GPx), hence preventing oxidative damage to tissues in the body [18].

Synthesis of Se-NPs can be achieved by a variety of methods including physical, chemical, and biological (green synthesis) as the most widely used [19]. Biological approaches that use microorganisms to produce Se-NPs are sustainable and cost-effective since they don't use harsh reaction conditions or produce harmful by-products [20]. More significantly, the biologically generated Se-NPs frequently showed excellent biocompatibility and stability without the need for capping or stabilizing chemicals [21].

Fungi have been shown to be more productive in producing nanoparticles than bacteria because they can secrete more proteins and amino acids [22]. It is technically possible for filamentous fungi to manufacture Se-NPs both extracellularly and intracellularly [28].The utilization of fungal supernatant facilitates more effective bioprocessing and biomass handling when compared to bacteria and other unicellular organisms [28].

In the present work, toxicity of the biogenic Se-NPs produced by *Penicillium citrinum* against hepatocellular carcinoma (HepG2) and lung carcinoma (A-459), as well as normal fibroblast cells (WI-38), was evaluated to determine their anticancer efficacy. Furthermore, cell cycle, apoptosis analysis as well as oxidative markers were also evaluated.

2. Materials and Methods

2.1. Fungal Strain

The biosynthesis of Se-NPs was carried out using *Penicillium citrinum*ATCC 36382.This fungal strain was maintained on Peptone Malt Dextrose Medium (PMD) (Biolab, Hungary) at 28 ± 2 °C for 3– 5 days.

2.2. Synthesis of Se-NPs

Peptone Malt Dextrose (PMD) broth Medium (150 mL / 250 mL Erlenmeyer flask) was inoculated with *Penicillium citrinum* and shacked at 100 rpm for 7 days at 25°C. The fungal growth was filteredthrough Whatman filter paper no. 1, and the fungal culture filtrate (FCF) was then used to reduce 10^5 ppmselenium oxide (Cambrian Chemicals Co.) with aratio of 1: 3and kept at roomtemperature for48hr. Concurrently, a negative control of non-inoculated broth culturemixed with selenium oxide solution, and was kept at the same conditions. After centrifugation at 20,000 rpm, the precipitated Se-NPs was twice washedwith distilled waterthen driedfor2hr at 80°C. Se-NP product was eventually collected and subjected for further investigation.

2.3. Characterization of Se-NPs

UV absorbance of the Se-NPs in the 200–700 nm range was measured using a scanning spectrophotometer (Shimadzu UV-spectrophotometer–1800, Japan) to determine its Surface Plasmon Resonance (SPR). Fourier Transform Infrared (FTIR) spectra was obtained using the NicoletTM iS50/R, FTIR, at 400–4000 cm^{-1}. The potential functional groups responsible for the reduction of selenium ions were found using FT-IR analysis. The biosynthesized nanoparticles' morphology and size were investigated using a Transmission Electron Microscope (TEM) on a JEOL GEM-1010, Japan. To determine the crystalline structure, an X-ray diffraction (XRD) pattern was recorded at 80 kV using a nickel filter and an X-ray diffractometer (Panalytical X` Pert Pro Netherlands) using Cu-Ka as the radiation source and a scanning speed of 2° min^{-1} in the 2θ from 4° to 70°.

2.4. Evaluation of Se-NPs cytotoxicity using cell viability assay

HepG2 (human hepatocellular carcinoma cells), A-549 (lung carcinoma cells), and WI-38 (normal fibroblasts cells) were obtained from VACSERA (Giza, Egypt). The cell lines were kept at 37ºC in a humidified 5% CO_2 incubator (Thermo Scientific, City, USA) in Dulbecco's modified Eagle's medium (DMEM) supplemented with 10% fetal bovine serum (Gibco, USA), 100 U/ml penicillin, and 100 µg/mL streptomycin.

For cytotoxicity assay [24], in a 96-well plate, 100 µL of growth media was seeded by 1×10^4 cells/ well. Using a multichannel pipette, confluent cell monolayers were distributed into 96-well flat-bottomed micro titre plates (Falcon, NJ, USA) and serial two-fold dilutions of the tested compound were added. The micro titre plates were incubated for 24hrat 37ºC in a humidified incubatorcontaining 5% CO_2.Three wells were used for each concentration ofthe tested samples and control cells. Viable cell yield was assessed using a colorimetrictechnique following incubation of the cells.

Once the incubation period was up, the media were removed and each well was flooded withcrystal violet solution (1%) for 30 min. After the stain was removed,the plates were rinsed with tap water to get rid of any remaining stain. Glacial acetic acid (30 %) was added to each well and mixed well,the plates were gently shaken on a Microplate Reader (TECAN, Inc.) to measure the absorbance at wavelength of 490 nm. Background absorbance found in wells without additional stain was taken into account when adjusting all results. In the absence of the investigated substances, treated samples were compared with the cell control. Every experiment was run in triplicate. To count the number of viable cells, the optical density was measured using a microplate reader (SunRise, TECAN, Inc., USA), and the percentage of viability was computed as $[(OD_t/OD_c)]x100$ where OD_t is the mean optical density of wells treated with the tested sample and OD_c is the mean optical density of untreated cells. The survival curve of each tumor cell line was obtained by plotting the relationship between remaining cells and drug concentration. Using graphic plots of the dose response curve for each conc., the cytotoxic concentration (CC_{50}), or the concentration needed to elicit toxic effects in 50% of intact cells, wasdetermined usingGraphpad Prism software (San Diego, CA, USA).

The selectivity index (S.I.) was calculated as the average of the IC_{50} value in the normal cell line (WI-38) divided by the IC_{50} value in the cancer cell line (A549) and (HepG2) obtained in each independent experiment [25].

.

2.5. Quantification of oxidative stress elements

HepG2 cells were seeded on 24-well tissue culture plates by 2.5×10^6 cells/well. After the formation of a complete monolayer cell sheet in each well of the plate, the obtained SeNPs were dispensed into the 24-well tissue culture plate (100.2 µg/mL). Each treatment was performed in triplicate. Following treatment, the culture medium was aspirated and the cells were collected from each well.

2.5.1Reduced glutathione (GSH) content

The method ofSiddiqui [**26**]was used with slight modifications in order to measure the intracellular GSH level.In brief, to obtain a full protein precipitation, 1 mL of the sonicated cell suspension was treated with 1 mL of 10% trichloroacetic acid (TCA) and cooled in ice for 1 hr. The mixture was then centrifuged for 10 min at 3000 rpm and the supernatant was mixed with 0.4 M Tris buffer (pH 8.9) containing 0.02 M ethylene diamine tetra-acetic acid (EDTA) and 0.01 M 5, 5'-dithionitrobenzoic acid (DTNB). Distilled water was then added to the mixture to get 3 mL final. Mixtures were incubated for 10 min at 37°C in a shacked water bath and absorbance of the produced yellow color was measured at 412 nm Using a microplate reader (SunRise, TECAN, Inc., USA.

2.5.2Catalase (CAT) enzyme activity

By following the manufacturer's instructions, BioDiagonstic kit (Diagnostic and research reagent) was used to, the activity of the catalase enzyme wasmeasured using the cell lysate of both the treated and untreated HepG2 cells after a 24-hr incubation period. Every sample was tested three times, and the concentrations were determined by plotting the standard curve

2.5.3Superoxide dismutase (SOD) activity

Using Kakkar's methodology [27], the SOD activity was determinedin a 3ml final volume containing 780 µM nicotinamide adenine dinucleotide (NADH), 0.052 M sodium pyrophosphate buffer (pH 8.3), 186 µM phenozine methosulphate (PMS), 300 µM nitro blue tetrazolium (NBT), sonicated enzyme preparation, and water.The reaction mixture was incubated at 37°C for 90 s, then glacial acetic acid (1mL)was added to stop the reaction, then strongly shacked with 4.0 mL of n-butanol. After centrifugation, the butanol layer was separated and the color intensity of the chromogen in butanol was measured at 560 nm in relation to butanol. A mixture that contained cell suspension but no enzyme was used as the control.

2.6Cell apoptosis assay

Using the Annexin V-FITC test (Becton Dickinson BD PharmingenTM, Heidelberg, Germany), cell apoptosis was measured in accordance with the

manufacturer's procedure. After HepG2 cells were cultured to a confluent monolayer, Se-NPs were added at the IC_{50} concentration. Following a 24-hr treatment period, the cells were removed and twice washed in PBS (20 min each), before being added to binding buffer (0.1M Hepes (pH 7.4), 1.4M NaCl, and 25 mM $CaCl_2$). Furthermore, HepG2 cells, whether they were treated or not, were re-suspended in 100 µL of kit binding buffer and 1 µL of FITC-Annexin V was added. This was done for 40 min at 4°C. After that, the cells were rinsed out and resuspended in 150 µL of binding buffer, to which 1 µL of 4′,6-diamidino-2-phenylindole (1 µg DAPI /mL in PBS, Invitrogen, Life Technologies, Darmstadt, Germany) was added. Using BD FACS Calibur flow cytometry (BD Biosciences, San Jose, CA), the percentage of living, apoptotic, and necrotic cells was determined [28].

2.7Cell cycle analysis using Flow Cytometry

The Cycle TEST TM PLUS DNA Reagent Kit (Becton Dickinson Immuno cytometry Systems, San Jose, CA) was used to carry out cell cycle analysis in order to ascertain the impact of the tested active samples on the cell cycle distribution of the HepG2 cell line. After being collected, the HepG2 cells—whether treated or not—were twice cleaned with cold PBS. 1 X 10^6 cells/ mL were the final concentration of the cell suspension. After overnight fixationin 100% ethanol at 4°C, the cells were re-suspended in 200 µL of 1X propidium iodide (PI), placed on ice bath and finally incubated for 20 - 30 min at 37°C in the dark.The populations of the G0/G1, S, and G2/M phases were identified using a PI detector and flow cytometry (Beckman Coulter, USA), and the results analysis were carried out using Cell Quest software (Becton Dickinson Immuno-cytometry Systems, San Jose, CA).

2.8Determination of the Caspase-3 using the Enzyme-linked immune sorbent assay (ELISA)

By following the manufacturer's instructions (BioSource, CA, USA), an ELISA kit was used to measure the activity of Caspase-3 in the treated and untreated HepG2 cell lysate after 24-hr incubation period. Every sample was tested three times, and the concentrations were determined by plotting the standard curve.

2.9Statistical Analysis

IBM SPSS Statistics 25 was used to analyze all of the obtainedexperimental data. The results weredisplayed as the average ± Standard Deviation (SD). To compare differences between groups, a two-tailed Student's t-test was employed. It was deemed statistically significant when $p < 0.05$.

3. Results and Discussion

3.1 Preparation and characterization of the SeNPs.

After being incubated at room temperature for 48 hr, the *P. citrnium* fungal culture filtrate (FCF)color waschanged to red (Fig. 1 A) when mixed with a selenium oxidesolution (10^5 ppm) in a ratio of 1: 3. Thisdeveloped red color was considered asindicator that *P. citrnium* has the capacity to form Se-NPs, which are a feature of monocolloidal Se-NPs as previously described [29]. The current study also supported the findings of Zare et al. [30], who used *Aspergillus terreus*to synthesize Se-NPs extracellularly. Fig. 1(B) displayed the produced Se-NPs' UV–visible spectrum. It showed a broad peak ranged from 240 to 265 nm and centered at 255.The UV spectra centered between 200 and 300 nm were due to the formation and surface plasmonvibration of Se-NPs [31]. Accordingly, this peak at 255 nm is corresponding to the surface plasmon resonance and indicating the formation of Se-NPs. This is consistent with the findings of Zare et al. [30], who proposed that a peak in the spectrum, corresponding to surface plasmon resonance and situated at 245 nm, indicated the formation of Se-NPs.This resultswere strongly agreed with Gharieb et al. [32], who found that the surface plasmon vibrations of Se-NPs was confirmed by the maximumUV–visible spectra absorption peak at 257 nm.

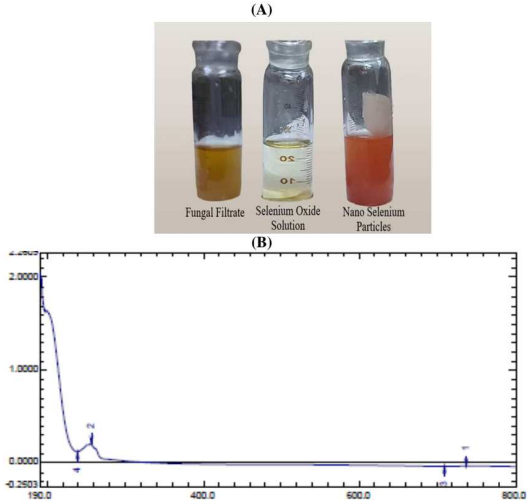

Figure 1: (A) Reduction to red elemental selenium "Se-NPs" by the filtrate of *P. citrinum* (B) UV–Vis spectrum

The FTIR spectrum of the Se-NPs produced from *P. citrnium* fungal culture filtrate (FCF) are displayed in Fig. 1 (C). The amide (-N-H) group was found to have a broad band at 3443.33 cm^{-1} [33], with the C–H group indicated by the broad peak at 2090.6 cm^{-1} and the CO group indicated by the broad peak at 1637 cm^{-1} [34]. The –CO and –N–H stretch vibrations in the protein amide bondsmay be the cause of these bands.The peak of the selenium metal was measured at 560 $cm^{-1}$was observed in FT-IR for Se-NPs and it refers to successful conjugation between the OH group and Se-NPs as Se–O [35]. The FTIR spectrum demonstrates how fungus-secreted proteins and enzymes contribute to the formation of Se-NPs. According to Srivastava[36], who proposed that extracellular proteins and enzymes secreted by fungi are responsible for the selenium reduction into Se-NPs and giving them their stability. These biomolecules are in charge of the reduction and long-term stability of biosynthesized Se-NPs Similarly these results agree with [32].In the low wavelength range, there appear amide I band at 1636 cm-^{1} (C=O stretch of the ester group).

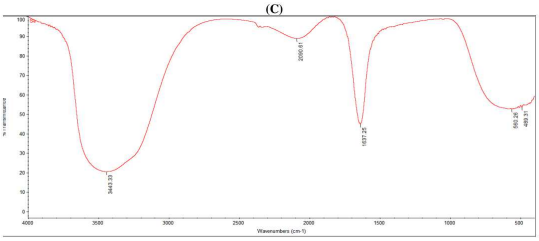

Figure 1: (C) FTIR spectrum of the Se-NPs produced from *P. citrnium* fungal culture filtrate

The crystallinity and crystalline size of the mycosynthesized SeNPs were studied by XRD analysis (Fig. 1 D).The diffraction peaks at 2θ = 23.5, 29.8, 41.4, 43.7, 45.4, 51.7, 55.9, 61.6 and 65.1 correspond to the (100), (101), (110), (102), (111), (201), (112), (202) and (210) reflections of pure hexagonal Se crystals (P3121). Scherer's formula was used to determine the average crystalline size of Se-NPs for peak 101. The biosynthesized Se-NPs had an average estimated crystalline size of 34.2 nm which agree with the results obtained by **[32].**

TEM was used to examine the morphology and microstructure of Se-NPs. The TEM images, Fig. 1(E),showed homogenous spherical Se-NPs, with sizes ranging from 15 to 40 nm and this agree with the results obtained by **Amin et al [37]** who stated that theTEM images of the myco-synthesized Se-NPs prepared by the fungal strain F9 biomass filtrate have size ranged between 3 nm to 15 nm with an average size of 7.3 ± 3.7 nm.

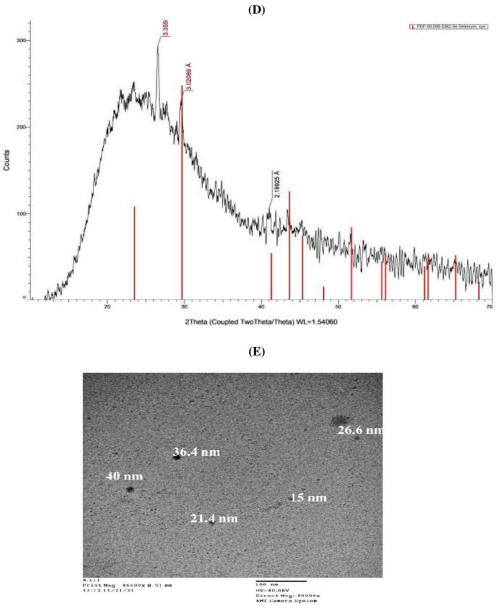

Figure 1: (D) XRD, and (E) TEM micrographs (100 nm scale) of the myco-synthesized Se-NPs

3.2 Evaluation of cytotoxicity of Se-NPs using viability assay

The toxicity of SeNPs was measured by the crystal violet assay and SeNP induced cell death in both cell lines. The result of the cytotoxicity is presented in Fig. 2. SeNPs induced cytotoxicity in HepG2 and A-549 cells in a dose-dependent manner, but more toxicity was observed in HepG2 cells than in A-549 cells (Fig. 2) as evidenced by their respective IC_{50} values of 100.2 ± 3.28 µg/mL and 142.5 ± 6.91 µg/mL. Se-NPs had an IC_{50} of 219.75±10.93 µg/mLagainst WI-38 cells.

Comparing Since selectivity is the most relevant parameter to detect anticancer potential *in vitro* [38,39], selectivity indices were used to quantify this parameter.

A molecule with moderate selectivity has a SI value greater than 2, whereas one with low selectivity is one whose SI value is less than 2 [40]. Se-NPs demonstrated a 2.19-fold increase in selectivity for HepG2 cells relative to WI-38 cells, indicating a moderate level of selectivity for HepG2. However, the SI for A-549 was 1.54-fold, showing a low level of selectivity.These results could be indicating the applicability of the SeNPs against HepG2.Thus, the use of Bio-SeNPs as anticancer agent may minimize the damage of chemotherapy by selective delivery to cancer cells without affecting human cells[41]the fabricated selenium nanoparticles are extremely safe and can be a promising candidate for safe materials for different applications[42].

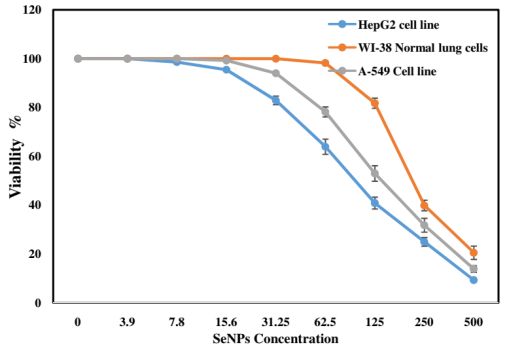

Figure 2: Cytotoxicity of the myco-synthesized Se-NPs against Human lung fibroblast normal cells "WI-38", Human Hepatic Carcinoma "HepG 2" and Lung carcinoma "A-549" cell line

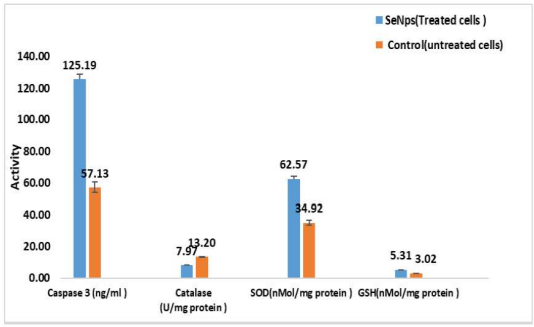

Figure 3: Myco-synthesized Se-NPs induced Caspase 3 activity, and oxidative stress biomarkers: Catalase, Super oxide dismutase "SOD "and Glutathione "GSH" in the HepG2 cell line.

3.3. Quantification of oxidative stress elements

NPs possess special characters (size, surface area, shape, solubility, and aggregation status) that associate with their capability to produce ROS [43**,** 44]**.**ROS has a major role in various cellular mechanisms, such as cell cycle, cell proliferation, and gene expression, and ultimately the mechanism of cell growth was stopped or cell death occurred [45]**.**

In this experiment, the generation of intracellular ROS showed itsproduction level increases in the HepG2 treated Cells. As shown in Fig. (3), theSOD level was considerably elevated in the Se-NPs treated HepG2 cells (62.57 nMol/mg), as compared to 34.92 nMol/mg protein in the untreated cells (approximately 1.8 fold). These results are in accordance with that obtained by [44], who mentioned an increase in the SOD level accompanied the oral treatment with SeNPs. Additionally, the treated HepG2 cells showed an increase in the GSH levels, from 3.02 nMol/mg the control sample to 5.31 nMol/mg (approximately 1.7 fold).

In addition, the liver's GSH content rose by roughly 65.24 % as compared to the untreated control. However, an unexpected result that catalase activity has dropped from 13.2 U/mg to 7.97 U/mg. On the contrary, in a study done by Bhattacharjee et al.(2019), the control group showed a 33.87 % increase in the content of catalase. The aforementioned findings imply that Se-NPs have a significant impact on changes in the oxidative stress response.

3.4. Se-NPs induced apoptosis, cell cycle arrest at G2/M and caspase-3 of HepG2 cells

One of the most significant mechanisms of selenium's anticancer action is thought to be apoptosis [45]. The cell apoptosis rates were measured using the Annexin V-FITC labelling technique in order to quantitatively evaluate the apoptosis induced by Se-NPs.

Nucleus of both necrotic and apoptotic cells can be stained by DAPI, a nucleic acid dye, even though it cannot pass through the intact cell membranes. Thus, to differentiate between early (Annexin V positive and DAPI negative) and late apoptosis (Annexin V/DAPI double positive), Annexin V and DAPI were be used in combination (**Fig. 4 A, B, and C**). Necrosis, late apoptosis, and early apoptosis rates were increased from 1.65 % to 14.85 % (9 folds), from 0.15 % to 8.27 (55 folds), and from 0.32 % to 11.61 % (36.3 folds) respectively when treated with Se-NPs with 100. 2 µg/ml (IC_{50}). These findings corroborated those of **[46]** who demonstrated that colon cancer cells (CT26) treated with nano-selenium had a higher population of apoptotic cells. In particular, the proportion of apoptotic cells increased from 8.89 % in the control sample to 13.5 % in the sample treated for 18 hr and finally to 28.1 % in the sample treated for 48 hr. Necrotic cell population was increased from 14.5 % (control sample) to 29.1 % (treated for 18 hr) and finally 40.3 % treated for 48 hr. These findings demonstrated that Se-NPs significantly promoted HepG2 cell death. Another study [47] using the CT26 colon cancer cell line showed that the percentages of pro-apoptotic and necrotic cells increased when the cells were treated with Se-NPs. Se-NPs have been shown in a study [48] using prostate cancer cell lines to have an anticancer effect on cancer cells by inducing enhanced apoptosis and cell cycle arrest.

In order to provide additional substantiation regarding the function of Se-NPs in augmenting apoptosis, the caspase-3 activity was evaluated subsequent to the exposure to IC_{50} (100.2 µg/mL) of Se-NPs. The results showed that as compared to the untreated control cells, the HepG2 cells treated with Se-NPs had 2.2 times greater Caspase 3 enzyme expression levels (**Fig. 3**). Similarly, **[49]**investigated how Se-NPs affected prostate LNCaP cancer cells, where Se-NPs significantly destroying ARs, which in turn caused caspase-mediated death. The level of activated caspase-3 in colorectal cell lines (HT26 and Caco-2) was assessed using a flow cytometry assay following treatment with Se-NPs made from the probiotic strain *Lactobacillus casei* ATCC393 [47].They demonstrated an induction of the caspase-3 level after Se-NPs treatment in a time-dependent manner. Also treating non-small cell lung cancer (NSCLC) cells (A-549 and NCI-H23) with nano-Se in combination with radiation, Tian et al. study[50]showed an increase in the expression levels of cleaved caspase-3 and cleaved caspase-9. A study using HepG2 and MCF7 breast cancer cells showed that treatment with Se-NPs increased the expression of caspase-3 mRNA by approximately 2.1 times compared to the control [51].Thus, our findings support the earlier research indicating that Se-NPs activated the caspase-3 enzyme to cause apoptosis in several cancer types.

Flow cytometry was used to track how SeNPs affected cell cycle arrest. The percentage of cells in the G1 phase dropped from 49.16 % to 44.57 %, the percentage of cells in the S phase dropped from 36.71 % to 31.52 %, and the percentage of cells in the G2/M phase increased from 14.1 % to 23.91 % relative to the control group (**Fig. 5**). These data suggest that chromatin condensation, chromosomal central alignment, and G2 checkpoint inactivation are disrupted. Consequently, at the G2/M phase, nano-Se stopped the cell cycle. These findings concur with those of [**52**], who discovered that Se-NPs dramatically slowed the development of A-549 cells by inducing G2/M phase arrest and death.

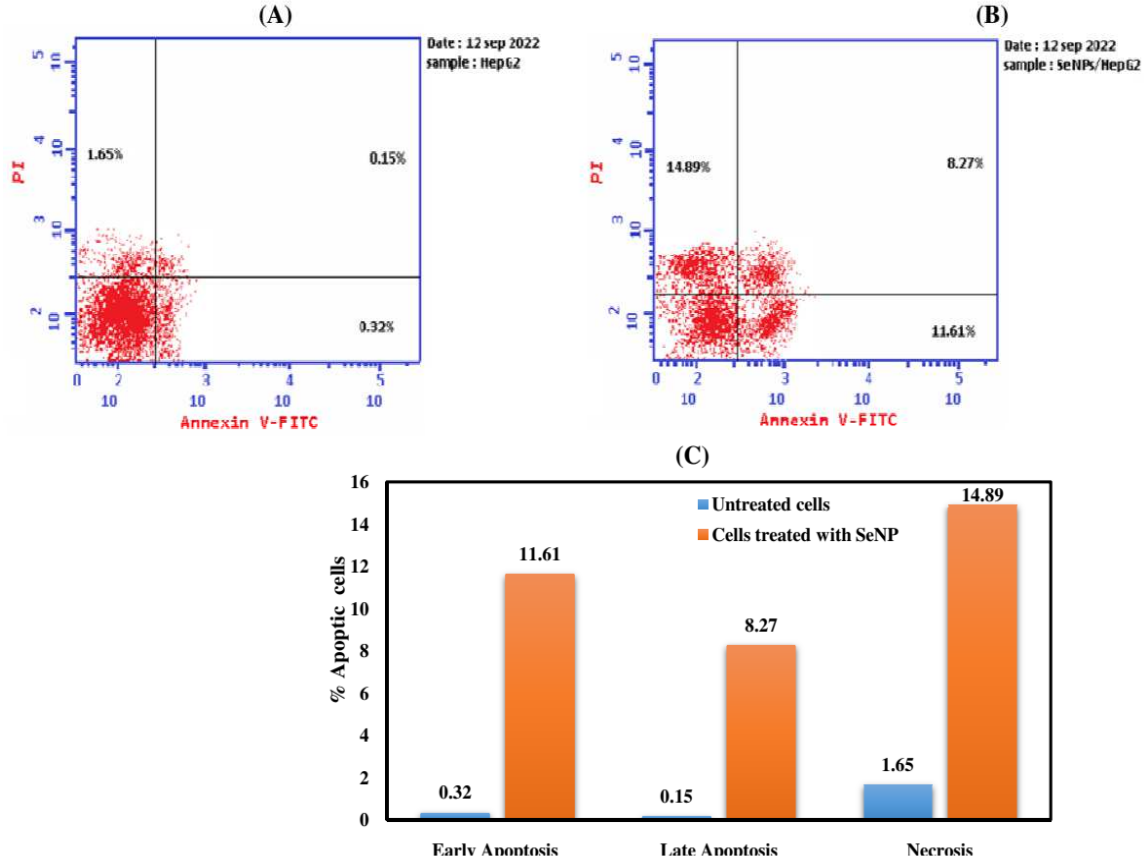

Figure 4: Flow cytometry dot plots of Annexin V-FITC/PI double staining for the detection of HepG2 cells apoptosis(Control)(A)and treated with SeNPs (100.2 µg/ml)(B) for the detection of cells apoptosis. (C)Percentage apoptotic cells induced by SeNPs-treated HepG2 cells.

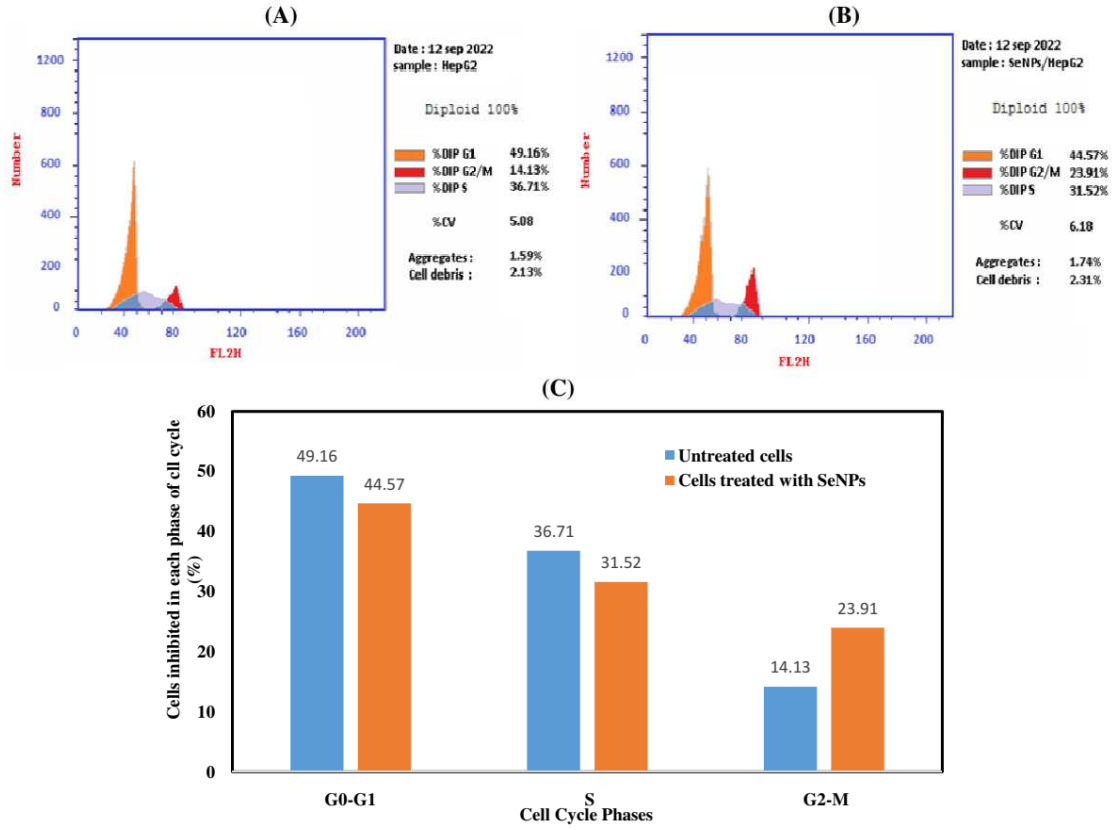

Figure 5: Cell Cycle analysis of untreated (A)and treated with SeNPs(B) HepG2 Cells that was done by using flow cytometry. (C)SeNPs enhance cell Cycle arrest and appearance G2/M Phase in HepG2 cells treated with Se-NPs at conc.100.2 µg/ml.

4. Conclusion

In conclusion, this study confirms the potentiality of the fungal strains, *P. citrinum* as a promising fungi for green synthesis of SeNPs in a spherical shape with a diameter ranging between 15 and 40 nm. Additionally, this work displayed anticancer activity against HepG2 and A-459 via enhancing apoptosis and antioxidant activity in addition to cell cycle arresting. Thus, the current study encourages working on scaling up the process of SeNP biosynthesis for cancer targeted therapy**.**

5. Conflicts of interest

The authors declare no conflict of interest.

6. Formatting of funding sources

No fund received to carry out this work.

7. Acknowledgments

The authors are sincerely thankful to Botany Department, Faculty of Women for Arts, Science and Education, Ain Shams University. The authors also thank Department of Industrial Biotechnology, Genetic Engineering and Biotechnology Research Institute, University of Sadat City, Cancer Biology.

8. Reference

[1]Tayel, A. A., Sorour, N. M., El-Baz, A. F., and Wael, F. (2017). Nanometals appraisal in food preservation and food-related activities. In *Food preservation* (pp. 487-526). Academic Press.

[2]Alsaggaf, M. S., Elbaz, A. F., El-baday, S., and Moussa, S. H. (2020). Anticancer and antibacterial activity of cadmium sulfide nanoparticles by *Aspergillus niger*. *Advances in Polymer Technology*, *2020*, 1-13.

[3] El-Baz, A.F. Sorour, N. M and Shetaia,Y. M. (2016).*Trichosporon jirovecii*-mediated synthesis

of cadmium sulfide nanoparticles.Journal of Basic Microbiology. 56 (5), 520 – 530.

[4]Hassan, A., Sorour, N. M., El-Baz, A., and Shetaia, Y. (2019). Simple synthesis of bacterial cellulose/magnetite nanoparticles composite for the removal of antimony from aqueous solution. *International journal of environmental science and technology*, *16*, 1433-1448.

[5] Shakweer, W. M. E., Azzaz, H. H., El-Nomeary, Y. A., El-Sayed, S. M., Youssef, A. M., & Hassaan, N. A. (2023). Synthesis and Characterization of Selenium Nanoparticles and its Effects on in vitro Rumen Feed Degradation, Ruminal Parameters, and Total Gas Production. Egyptian Journal of Chemistry, 66(12), 189-197.

[6] Cong, W., Bai, R., Li, Y. F., Wang, L., & Chen, C. (2019). Selenium nanoparticles as an efficient nanomedicine for the therapy of Huntington's disease. *ACS applied materials & interfaces*, *11*(38), 34725-34735.

[7] Johnson, J. A., Saboungi, M. L., Thiyagarajan, P., Csencsits, R., & Meisel, D. (1999). Selenium nanoparticles: a small-angle neutron scattering study. *The Journal of Physical Chemistry B*, *103*(1), 59-63.

[8] Vidal, O., Goffé, B., & Arndt, N. (2013). Metals for a low-carbon society. Nat. Geosci. 6 (11), 894–896.

[9] Khoei, N. S., Lampis, S., Zonaro, E., Yrjälä, K., Bernardi, P., & Vallini, G. (2017). Insights into selenite reduction and biogenesis of elemental selenium nanoparticles by two environmental isolates of Burkholderia fungorum. *New biotechnology*, *34*, 1-11.

[10]Halwani, A. A. (2022). Development of pharmaceutical nanomedicines: from the be
nch to the market. *Pharmaceutics*, *14*(1), 106.

[11]Baranwal, J., Barse, B., Di Petrillo, A., Gatto, G., Pilia, L., and Kumar, A. (2023). Nanoparticles in cancer diagnosis and treatment. *Materials*, *16*(15), 5354.

[12]Dessale, M., Mengistu, G., and Mengist, H. M. (2022). Nanotechnology: a promising approach for cancer diagnosis, therapeutics and theragnosis. *International Journal of Nanomedicine*, *17*, 3735.

[13]Giannitrapani, L., Soresi, M., Bondì, M. L., Montalto, G., and Cervello, M. (2014). Nanotechnology applications for the therapy of liver fibrosis. *World journal of gastroenterology: WJG*, *20*(23), 7242.

[14]Wang, H., Zhang, J., and Yu, H. (2007). Elemental selenium at nano size possesses lower toxicity without compromising the fundamental effect on selenoenzymes: comparison with selenomethionine in mice. *Free Radical Biology and Medicine*, *42*(10), 1524-1533.

[15] Ahmed, K. B. A., Kalla, D., Uppuluri, K. B., and Anbazhagan, V. (2014). Green synthesis of silver and gold nanoparticles employing levan, a biopolymer from Acetobacter xylinum NCIM 2526, as a reducing agent and capping agent. *Carbohydrate polymers*, *112*, 539-545.

[16]Chen, W., Cheng, H., and Xia, W. (2022). Progress in the surface functionalization of selenium nanoparticles and their potential application in cancer therapy. *Antioxidants*, *11*(10), 1965.

[17] Cheng, L., Wang, Y., He, X., and Wei, X. (2018). Preparation, structural characterization and bioactivities of Se-containing polysaccharide: A review. *International journal of biological macromolecules*, *120*, 82-92..

[18] Horky, P., Ruttkay-Nedecky, B., Nejdl, L., Richtera, L., Cernei, N., Pohanka, M., and Adam, V. (2016). Electrochemical methods for study of influence of selenium nanoparticles on antioxidant status of rats. *International Journal of Electrochemical Science*, *11*(4), 2799-2824.

[19]Venugopal, S. (2022). Therapeutic potential of selenium nanoparticles. *Frontiers in Nanotechnology*, *4*, 1042338.

[20] Truong LB, Medina-Cruz D, Mostafavi E, Rabiee N. Selenium nanomaterials to combat antimicrobial resistance. Molecules. 2021;26:3611.

[21] Gavamukulya, Y., Maina, E. N., Meroka, A. M., Madivoli, E. S., El-Shemy, H. A., Wamunyokoli, F., and Magoma, G. (2020). Green synthesis and characterization of highly stable silver nanoparticles from ethanolic extracts of fruits of Annona muricata. *Journal of Inorganic and Organometallic Polymers and Materials*, *30*(4), 1231-1242.

[22]Hulkoti, N. I.,and Taranath, T. C. (2014). Biosynthesis of nanoparticles using microbes—a review. *Colloids and surfaces B: Biointerfaces*, *121*, 474-483.

[23]Liang, X., Zhang, S., Gadd, G. M., McGrath, J., Rooney, D. W., & Zhao, Q. (2022). Fungal-derived selenium nanoparticles and their potential applications in electroless silver coatings for preventing pin-tract infections. *Regenerative biomaterials*, *9*, rbac013.

[24]Mosmann, T. (1983). Rapid colorimetric assay for cellular growth and survival: application to proliferation and cytotoxicity assays. *Journal of immunological methods*, *65*(1-2), 55-63.

[25]Abdelaal, M. R., Soror, S. H., Elnagar, M. R., & Haffez, H. (2021). Revealing the potential application of EC-synthetic retinoid analogues in anticancer therapy. *Molecules*, *26*(2), 506.

[26]Siddiqui, M. A., Kashyap, M. P., Kumar, V., Al-Khedhairy, A. A., Musarrat, J., and Pant, A. B. (2010). Protective potential of trans-resveratrol against 4-hydroxynonenal induced damage in PC12 cells. *Toxicology in vitro*, *24*(6), 1592-1598

[27] Kakkar P, Das B, Viswanathan PN. A modified spectrophotometric assay of superoxide dismutase. 1984;

[28] Lakshmanan, I., & Batra, S. K. (2013). Protocol for apoptosis assay by flow cytometry using annexin V staining method. *Bio-protocol*, *3*(6), e374-e374.

[29] Vieira, A. P., Stein, E. M., Andreguetti, D. X., Cebrián-Torrejón, G., Doménech-Carbó, A., Colepicolo, P., and Ferreira, A. M. D. (2017). " Sweet Chemistry": a Green Way for Obtaining Selenium Nanoparticles Active against Cancer Cells. *Journal of the Brazilian Chemical Society*, *28*, 2021-2027.

[30] Zare, B., Babaie, S., Setayesh, N and Shahverdi, A. R. (2013). Isolation and characterization of a fungus for extracellular synthesis of small selenium nanoparticles. *Nanomedicine journal*, *1*(1), 13-19.

[31]Hussein, H. G., El-Sayed, E. S. R., Younis, N. A., Hamdy, A. E. H. A., and Easa, S. M. (2022). Harnessing endophytic fungi for biosynthesis of selenium nanoparticles and exploring their bioactivities. AMB Express, 12(1), 68.

[32] Gharieb, M. M., Soliman, A. M., & Omara, M. S. (2023). Biosynthesis of selenium nanoparticles by potential endophytic fungi Penicillium citrinum and Rhizopus arrhizus: characterization and maximization. *Biomass Conversion and Biorefinery*, 1-10.

[33]Jabs, A. (2008). Determination of secondary structure in proteins by FTIR spectroscopy. *Jena Library of Biological Macromolecules*.

[34] Naidoo, C., Kruger, C. A., and Abrahamse, H. (2019). Targeted photodynamic therapy treatment of in vitro A375 metastatic melanoma cells. *Oncotarget*, *10*(58), 6079.

[35]Salem, S. S., Fouda, M. M., Fouda, A., Awad, M. A., Al-Olayan, E. M., Allam, A. A., and Shaheen, T. I. (2021). Antibacterial, cytotoxicity and larvicidal activity of green synthesized selenium nanoparticles using *Penicillium corylophilum*. *Journal of Cluster Science*, *32*, 351-361.

[36] Srivastava, N., and Mukhopadhyay, M. (2015). Biosynthesis and structural characterization of selenium nanoparticles using Gliocladium roseum. *Journal of Cluster Science*, *26*, 1473-1482.

[37] Amin, M. A., Ismail, M. A., Badawy, A. A., Awad, M. A., Hamza, M. F., Awad, M. F., and Fouda, A. (2021). The Potency of fungal-fabricated selenium nanoparticles to improve the growth performance of Helianthus annuus L. and control of cutworm Agrotis ipsilon. *Catalysts*, *11*(12), 1551.

[38] López-Lázaro M. (2015). Two preclinical tests to evaluate anticancer activity and to help validate drug candidates for clinical trials. Oncoscience, 2(2):91.

[39]López-Lázaro, M. (2015). How many times should we screen a chemical library to discover an anticancer drug? *Drug Discovery Today*, *2*(20), 167-169.

[40] Indrayanto, G., Putra, G. S., & Suhud, F. (2021). Validation of in-vitro bioassay methods: Application in herbal drug research. *Profiles of drug substances, excipients and related methodology*, *46*, 273-307.

[41]Abbas, H., & Abou Baker, D. (2020). Biological evaluation of selenium nanoparticles biosynthesized by Fusarium semitectum as antimicrobial and anticancer agents. *Egyptian Journal of Chemistry*, *63*(4), 1119-1133

[42] Shakweer, W. M. E., Azzaz, H. H., El-Nomeary, Y. A., El-Sayed, S. M., Youssef, A. M., & Hassaan, N. A. (2023). Synthesis and Characterization of Selenium Nanoparticles and its Effects on in vitro Rumen Feed Degradation, Ruminal Parameters, and Total Gas Production. *Egyptian Journal of Chemistry*, *66*(12), 189-197.

[43] Nel, A., Xia, T., Madler, L., & Li, N. (2006). Toxic potential of materials at the nanolevel. *science*, *311*(5761), 622-627

[44] Ray, P. C., Yu, H., & Fu, P. P. (2009). Toxicity and environmental risks of nanomaterials: challenges and future needs. *Journal of Environmental Science and Health Part C*, *27*(1), 1-35.

[45] Almutairi, B., Albahser, G., Almeer, R., Alyami, N. M., Almukhlafi, H., Yaseen, K. N., ... & Alarifi, S. (2020). Investigation of cytotoxicity apoptotic and inflammatory responses of biosynthesized zinc oxide nanoparticles from ocimum sanctum linn in human skin keratinocyte (hacat) and human lung epithelial (A549) cells. *Oxidative Medicine and Cellular Longevity*, *2020*.

[46] Bhattacharjee, A., Basu, A., and Bhattacharya, S. (2019). Selenium nanoparticles are less toxic than inorganic and organic selenium to mice in vivo. *The Nucleus*, *62*, 259-268.

[47] Shehata, N. S., Elwakil, B. H., Elshewemi, S. S., Ghareeb, D. A., and Olama, Z. A. (2023). Selenium nanoparticles coated bacterial polysaccharide with potent antimicrobial and anti-lung cancer activities. *Scientific Reports*, *13*(1), 21871.

[48]Iatroudi, A. Growth-inhibitory effects of biogenic nano-selenium in colon cancer cells.

[49] Spyridopoulou, K., Aindelis, G., Pappa, A.,and Chlichlia, K. (2021). Anticancer activity of biogenic selenium nanoparticles: apoptotic and immunogenic cell death markers in colon cancer cells. *Cancers*, *13*(21), 5335.

[50]Liao, G., Tang, J., Wang, D., Zuo, H., Zhang, Q., Liu, Y., and Xiong, H. (2020). Selenium nanoparticles (SeNPs) have potent antitumor activity against prostate cancer cells through the upregulation of miR-16. *World Journal of Surgical Oncology*, *18*, 1-11..

[51] Kong, L., Yuan, Q., Zhu, H., Li, Y., Guo, Q., Wang, Q., ... and Gao, X. (2011). The suppression of prostate LNCaP cancer cells growth by Selenium nanoparticles through Akt/Mdm2/AR controlled apoptosis. *Biomaterials*, *32*(27), 6515-6522.

[52] Tian, J., Wei, X., Zhang, W., and Xu, A. (2020). Effects of selenium nanoparticles combined with radiotherapy on lung cancer cells. *Frontiers in Bioengineering and Biotechnology*, *8*, 598997.

[53] Alkhudhayri, A., Al-Shaebi, E. M., Qasem, M. A., Murshed, M., Mares, M. M., Al-Quraishy, S., and Dkhil, M. A. (2020). Antioxidant and anti-apoptotic effects of selenium nanoparticles against murine eimeriosis. *Anais da Academia Brasileira de Ciências*, *92*, e20191107.

[54] Wu, H., Zhu, H., Li, X., Liu, Z., Zheng, W., Chen, T., .and Wong, K. H. (2013). Induction of apoptosis and cell cycle arrest in A549 human lung adenocarcinoma cells by surface-capping selenium nanoparticles: an effect enhanced by polysaccharide–protein complexes from Polyporus